Proceedings of the 4th International Conference on Mechatronics and Smart Systems
DOI: 10.54254/2755-2721/2026.35766

A Method for Diagnosing Transformer Faults under Online Voltage Signals

Zihao Zhong

School of Control and Information Engineering, Northeast Forestry University, Harbin, China
1528877528@qq.com

Abstract. Transformer degradation is often accompanied by changes in electrical characteristics. Such changes may originate from insulation defects, winding abnormalities, or local dielectric damage. Detecting these variations at an early stage remains a challenge for condition monitoring. In this work, primary-side and secondary-side power-frequency voltages were analyzed through U_1–U_2 Lissajous trajectories. Ellipse parameters, including the major axis, minor axis, and inclination angle, were extracted from the trajectories and used for comparison under different operating conditions. A transformer equivalent circuit was established, and impedance variations were introduced to represent abnormal states. Trajectory geometry changed continuously as the equivalent parameters varied. Among the extracted features, the inclination angle showed the largest variation. Noticeable differences were already present when the impedance deviation reached ±3%. The obtained results indicate that voltage trajectories contain information related to internal parameter changes and may be used for condition evaluation during operation. Since only terminal voltage measurements are required, the method can be implemented without additional sensing devices.

Keywords: fault, voltage signal, diagnosis method, curves

1. Introduction

Power transformers are indispensable components of modern transmission and distribution networks. Their operating state is closely related to the continuity and quality of power delivery. During long-term service, insulation systems, windings, and magnetic components are subjected to electrical stress, temperature rise, vibration, and electromagnetic forces. The effects of these factors are often cumulative rather than immediate. As a result, gradual changes may develop inside the equipment before obvious symptoms appear at the system level.

In practical operation, many abnormalities evolve slowly. A slight insulation defect or a small winding displacement may not cause noticeable changes in output performance. Utilities therefore face a familiar problem: equipment can remain in service while internal degradation continues to accumulate. Once the degradation reaches a certain level, the risk profile changes rapidly. Short-circuit events are a typical example. Large electromagnetic forces generated during such events may distort winding structures and aggravate existing weaknesses. Repair work can be time-consuming, and unexpected outages often lead to additional operational costs [1].

DOI: 10.54254/2755-2721/2026.35766

For this reason, transformer condition assessment has been studied for decades. Frequency Response Analysis (FRA) is widely used for winding evaluation [2]. Sweep Frequency Response Analysis (SFRA) extends this idea by examining responses over a broad frequency range [3]. Short-circuit impedance testing [4] and low-voltage impulse methods [5] are also well established in engineering practice. These techniques have contributed substantially to transformer diagnostics. A common feature, however, is that measurements are usually performed when the unit is removed from normal service. In large power networks, arranging such tests is not always straightforward.

Attempts to obtain diagnostic information during operation have led to a variety of online monitoring approaches. Ultrasonic inspection and vibration analysis are among the most frequently reported examples. Feng et al. introduced coded excitation and pulse-compression techniques into ultrasonic measurements [6]. Gao et al. investigated structural responses under short-circuit conditions using vibration-based models [7]. Valuable information can be obtained from these approaches. Nevertheless, practical deployment often requires dedicated sensors, signal-conditioning units, and additional acquisition hardware. Measurement quality may also depend on installation conditions and environmental influences [8-11].

Electrical quantities measured at transformer terminals provide another source of information. Unlike acoustic or vibration signals, they are directly associated with the electromagnetic behavior of the device. Several studies have explored trajectory-based analysis using Lissajous figures constructed from operating data [12-15]. Most reported work has concentrated on voltage-current trajectories or current-related features. Comparatively fewer studies have examined relationships between primary-side and secondary-side voltages [16-20]. Whether useful diagnostic information can be extracted from such voltage trajectories remains an open question [21-24].

The present work investigates this issue from the perspective of voltage trajectory characteristics. A transformer equivalent circuit was developed in Multisim, and different operating states were represented through parameter variations. Primary-side and secondary-side voltages were then processed in MATLAB to generate U_1–U_2 Lissajous trajectories. Ellipse fitting was performed for each trajectory, and three geometric quantities—the major axis, minor axis, and inclination angle—were selected for analysis. Their variation under different disturbance levels was examined. The results indicate that trajectory geometry changes systematically with equivalent parameter variation, with the inclination angle showing the largest response among the investigated features. Because the procedure relies only on voltage quantities already available at transformer terminals, no additional sensing hardware is required.

2. Model and method

2.1. Model development

A transformer can be represented by a two-port equivalent circuit. The model is used to describe the electrical relationship between the primary and secondary windings. Primary-side and secondary-side voltages are selected as the observation variables. The corresponding equivalent circuit is shown in Fig. 1 [25-27].

DOI: 10.54254/2755-2721/2026.35766

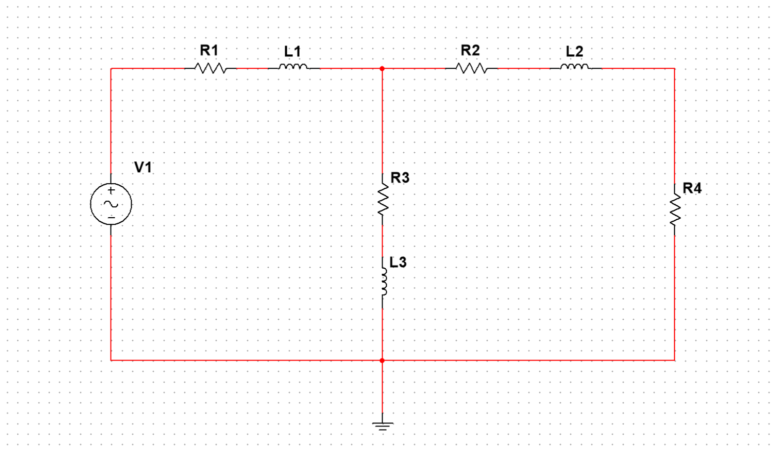

Figure 1. Equivalent circuit diagram of a transformer

Let μ_1 and μ_2 denote the instantaneous voltages of the primary and secondary sides. U_1 and U_2 are the corresponding voltage amplitudes. The supply frequency is represented by f, and φ_1 and φ_2 denote the initial phase angles. Under normal operating conditions, the voltage signals can be expressed as

$$\mu_1(t) = U_1 sin(2\pi ft + \varphi_1) \tag{1}$$

$$\mu_2(t) = U_2 sin(2\pi ft + \varphi_2) \tag{2}$$

The voltage relationship is governed by the electromagnetic coupling between the two windings. Transformer parameters determine both the voltage magnitude and phase characteristics. Changes in insulation condition, winding structure, or dielectric properties may modify the equivalent circuit parameters. Such changes are reflected in the measured voltage waveforms through amplitude variation or phase deviation.

2.2. Voltage trajectory method

Two harmonic signals with identical frequencies produce an elliptical trajectory in a Cartesian coordinate system [28-30]. The shape of the ellipse varies with signal amplitude and phase difference.

For the transformer considered in this work, primary-side voltage and secondary-side voltage are selected as the coordinate variables. The resulting trajectory is represented in the U_1–U_2 plane. Since both voltages originate from the same power-frequency source, an elliptical pattern is obtained under normal operating conditions.

The trajectory is characterized through ellipse fitting. Three geometric quantities are extracted, namely the major axis, minor axis, and inclination angle. These quantities describe differences in voltage magnitude and phase relationship between the two sides of the transformer.

Changes inside the transformer affect the corresponding equivalent parameters. Such changes modify the voltage relationship across the two ports and lead to observable variations in the fitted ellipse. Deviations in geometric features can therefore be used to distinguish different operating

DOI: 10.54254/2755-2721/2026.35766

states. The extracted geometric parameters therefore provide a convenient means of describing transformer condition.

Only voltage measurements are required during implementation. No additional excitation source or external sensing device is involved. All diagnostic information is obtained from the voltage relationship between the transformer terminals.

Only the single-phase case is considered in this work. The corresponding model is sufficient for examining the trajectory characteristics discussed in the following sections. Extension to other winding arrangements remains possible and is not addressed here.

3. Simulation model development and results

3.1. Simulation model

A transformer equivalent circuit was established in the simulation environment to study the relationship between terminal voltage characteristics and transformer condition. Figure 2 shows the simulation circuit. Primary-side and secondary-side voltages are monitored during the calculation process [31-34].

Model parameters are listed in Table 1. A 220 V, 50 Hz source supplies the circuit. R1–L1 and R2–L2 represent winding branches. R3–L3 represents the excitation branch. R4 is used as the load.

Parameter variations are introduced into R1, L1, R2, and L2. Three levels are considered: ±3%, ±5%, and ±10%. Positive and negative deviations are both included.

Rather than constructing separate models for individual faults, parameter variation is applied directly to the equivalent circuit. The resulting voltage signals are used for subsequent trajectory analysis [35-38].

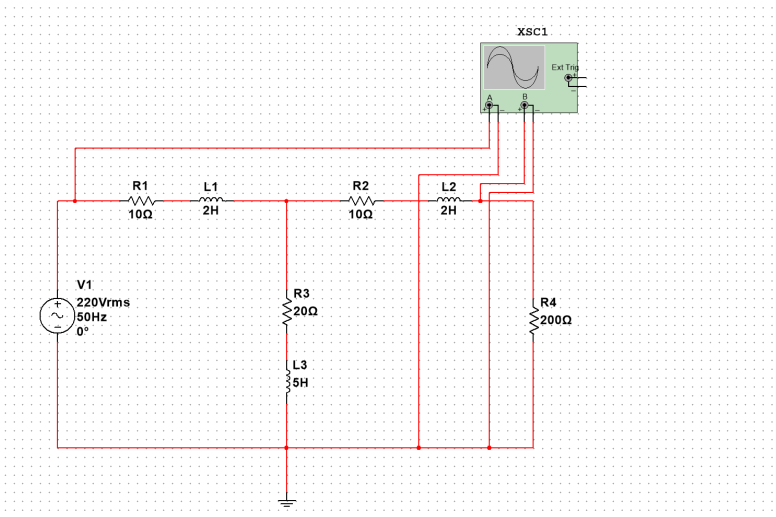

Figure 2. Two-port simulation model

Table 1. Components in the simulation diagram

Component	Component Function
Power Supply V1 (220 V/50 Hz)	Power source applied to the primary side of the transformer for power frequency testing

DOI: 10.54254/2755-2721/2026.35766

Table 1. (continued)

R1 (10Ω) + L1 (2H) series branch	Equivalent parameters of the transformer primary winding
R2 (10 Ω) + L2 (2 H) series branch	Equivalent parameters of the transformer's secondary winding
R3 (20 Ω) + L3 (5 H) parallel branch	Equivalent parameters of the transformer excitation branch (core + main flux)
R4 (200 Ω) load	External load on the transformer's secondary side (simulating actual operating/test conditions)

3.2. Analysis of simulation results

Primary-side and secondary-side voltage signals were obtained from the simulation model under normal and disturbed conditions. Parameter deviations of ±3%, ±5%, and ±10% were introduced into the equivalent circuit. The corresponding U_1–U_2 trajectories are presented in Figs. 3–5.

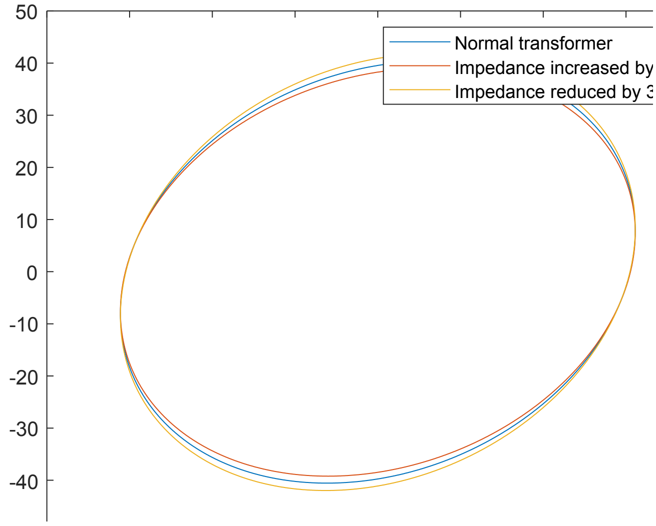

Figure 3. U_1–U_2 trajectory under normal conditions and ±3% impedance variation

The normal operating state produces an elliptical trajectory. Changes appear after parameter adjustment. The trajectory obtained under ±3% deviation remains close to the normal case. A wider separation is visible for ±5% deviation. The difference becomes more evident at ±10%.

The geometric characteristics of the trajectories vary with parameter deviation. Changes can be identified in ellipse size and orientation. The fitted major axis, minor axis, and inclination angle no longer coincide with those of the normal state.

Trajectories associated with different parameter levels occupy different regions in the U_1–U_2 plane. No overlap is found within the investigated range. Disturbance levels of ±3%, ±5%, and ±10% can therefore be distinguished from one another through trajectory geometry.

DOI: 10.54254/2755-2721/2026.35766

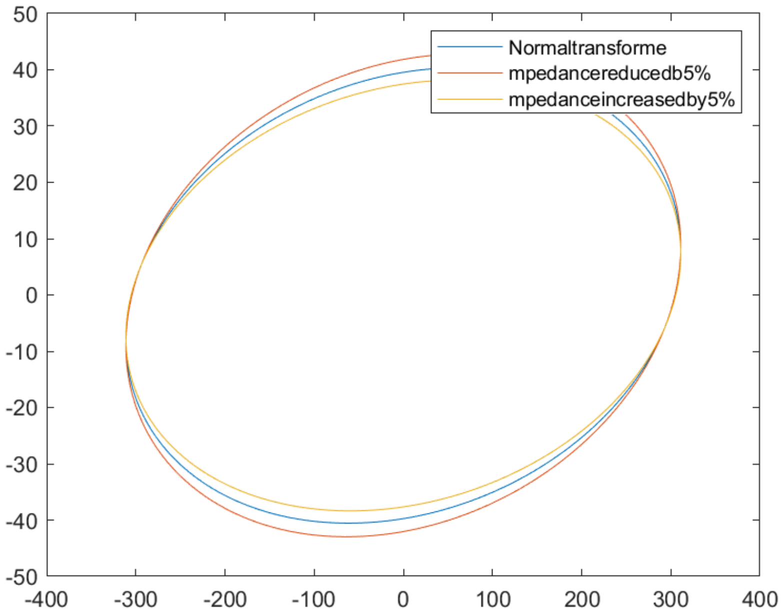

Figure 4. U_1–U_2 trajectory under normal conditions and ±5% impedance variation

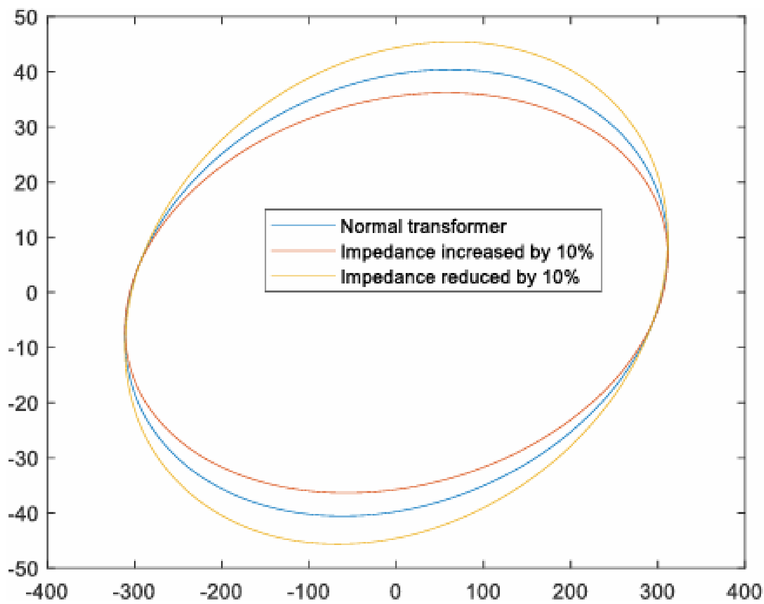

Figure 5. Lissajous figures for a normal transformer and one with a 10% change in impedance

4. Analysis of lissajous feature parameters

The trajectories shown in Figs. 3–5 were fitted using an ellipse model. Three geometric quantities were extracted from each trajectory: major axis, minor axis, and inclination angle. The corresponding values are listed in Table 2.

Different responses are observed among the three parameters. Only small changes occur in the major axis over the investigated range. Larger variations appear in the minor axis and inclination angle. Both parameters change continuously as the disturbance level increases.

Relative deviations with respect to the normal condition are summarized in Table 3. The major axis shows limited variation. The minor axis and inclination angle change more noticeably. Under

DOI: 10.54254/2755-2721/2026.35766

±10% disturbance, the relative variation exceeds 10% for both quantities.

Among the extracted parameters, the inclination angle shows the largest variation. For the ±3% case, the relative change is close to 5%. The corresponding value increases further as the disturbance level rises.

A relative deviation of 5% is used as the criterion in the present study. Values above this level are classified as abnormal.

Positive and negative parameter deviations produce opposite trends. Higher equivalent parameter values correspond to lower minor-axis and inclination-angle values. The reverse relationship appears when the equivalent parameters decrease.

Within the investigated interval, the minor axis and inclination angle change approximately in proportion to disturbance magnitude. Similar trends are observed for both positive and negative deviations.

Table 2. Comparison of lissarou figure elliptical eigenvalues

	Major Axis	Short Axis	Angle of inclination	Severity of failure
Normal transformer	880.2985	112.168	1.5009°	No fault
Increase of 3%	880.2665	108.5613	1.4170°	Minor failure
Increase by 5%	880.2475	106.2649	1.3649°	Major failure
Increase of 10%	880.207	100.8707	1.2465°	Severe failure
Decrease by 3%	880.3355	115.9833	1.5925°	Minor failure

Table 3. Percentage change in lissajous figure elliptical eigenvalues under different conditions

	Major axis	Minor axis	Inclination angle	
Increase of 3%	0.0036%	3.2154%	5.5900%	Increase of 3%
Increase by 5%	0.0058%	4.9985%	9.0612%	Increase by 5%
Increase by 10%	0.0139%	10.0718%	16.9498%	Increase by 10%
Decrease by 3%	-0.0042%	-3.4014%	-6.1030%	Decrease by 3%
Decrease by 5%	-0.0074%	-5.7800%	-10.4870%	Decrease by 5%

Another observation concerns the symmetry of the results. Positive and negative disturbances produce nearly opposite responses. When the equivalent parameters increase, the minor axis and inclination angle decrease. When the equivalent parameters decrease, both quantities increase. This trend remains visible throughout the investigated range. Such symmetry is beneficial because it indicates that the extracted features not only reflect the magnitude of parameter deviation but also contain information regarding the direction of change. In other words, the trajectory characteristics may provide clues about whether the equivalent impedance has increased or decreased relative to the normal condition.

It should also be noted that the present analysis focuses on relatively small parameter variations. Under actual operating conditions, transformer characteristics may be influenced by temperature fluctuations, loading conditions, manufacturing tolerances, and measurement noise. These factors were not explicitly considered in the simulation model. Even so, the extracted trajectory features continue to exhibit clear and consistent trends. This observation suggests that the geometric parameters are not responding randomly. Instead, they remain closely linked to the underlying electrical characteristics represented by the equivalent circuit.

DOI: 10.54254/2755-2721/2026.35766

Taken together, the results indicate that different ellipse parameters contribute differently to transformer condition assessment. The major axis remains comparatively stable, whereas the minor axis and inclination angle exhibit more pronounced responses. Among the investigated quantities, the inclination angle appears to provide the clearest indication of parameter variation. These observations provide additional support for selecting the minor axis and inclination angle as primary indicators in the subsequent evaluation of transformer operating conditions.

5. Conclusions

The relationship between primary-side and secondary-side power-frequency voltages was investigated through Lissajous trajectories derived from a transformer equivalent circuit model. Equivalent impedance was adjusted to represent different operating conditions. Corresponding changes appeared in the U_1–U_2 trajectories.

Only limited variation was observed in the major axis over the investigated range. The situation was different for the minor axis and the inclination angle. Once the equivalent impedance was adjusted, both quantities changed noticeably. Even in the ±3% cases, departures from the reference values could already be identified. Among the three extracted features, the inclination angle showed the most obvious response.

Another point worth noting is that the direction of parameter variation was reflected in the trajectory features. When the equivalent impedance increased, the minor axis and inclination angle generally became smaller. When the impedance decreased, the opposite tendency appeared. This pattern was observed repeatedly during the simulation process. Within the investigated interval, no abrupt jumps or irregular fluctuations were found, and the feature values changed in a relatively regular manner as the disturbance level increased.

The observations reported here come from a simulation study based on an equivalent transformer circuit. Real transformers are usually affected by manufacturing differences, operating environments, measurement noise, and many other factors that are difficult to reproduce completely in simulation. For this reason, experimental verification remains necessary. Future work will focus on laboratory measurements and practical operating data. It would also be useful to examine how the proposed trajectory features compare with results obtained from FRA, short-circuit impedance tests, and vibration-based diagnostic approaches under the same conditions.

References

[1] Kim, D. J., Park, J., Hong, Y., et al. (2026). Fault-tolerant independent pole control scheme of zigzag MMC for bipolar MVDC distribution systems. *IEEE Transactions on Power Electronics, 41*(6), 10324–10342.
[2] Ye, Z., Jia, H., Cai, W., et al. (2024). A new method of transformer short-circuit impedance regulation based on magnetic shunts. *Energies, 17*(15), 3714.
[3] Rajamani, R., Rajagopalan, M., & Madanmohan, B. (2017). Sweep frequency response analysis-based diagnosis of shorts within transformer windings. *IET Generation, Transmission & Distribution, 11*(11), 4274–4281.
[4] Bagheri, M., Naderi, M. S., Blackburn, T., et al. (2013). Frequency response analysis and short-circuit impedance measurement in detection of winding deformation within power transformers. *IEEE Electrical Insulation Magazine, 29*(3), 33–40.
[5] Zhang, Q., Xiang, B., Ma, S. X., et al. (2026). Load recovery performances of variable impedance superconducting fault current limiting transformers. *IEEE Transactions on Applied Superconductivity, 36*(5), 5500306.
[6] Feng, Y., Du, H. Y., Li, Y. M., et al. (2020). Transformer winding deformation detection technology based on pulse-coded excitation ultrasonic spread spectrum distance measurement. *High Voltage Apparatus, 56*(11), 0–0.
[7] Gao, S., Sun, L., Tian, Y., et al. (2022). Study on axial vibration distribution characteristics of transformers under short-circuit conditions considering damping parameters. *Applied Sciences, 12*(17), 8443.

[8] Senobari, R. K., Kakolaki, S. E. H., Sadeh, J., et al. (2025). Comprehensive experimental study on a wound-rotor asynchronous machine fault detection through frequency response analysis. *International Journal of Electrical Power & Energy Systems, 170*, 110852.
[9] Kubojima, Y., Sonoda, S., & Kato, H. (2018). Practical techniques for the vibration method with additional mass: Bending vibration generated by tapping cross section. *Journal of Wood Science, 64*(1), 16–22.
[10] Asl, M. B., Fofana, I., & Meghnefi, F. (2025). Comprehensive review of transformer winding diagnostics: Integrating frequency response analysis with machine learning approaches. *Energies, 18*(5), 1209.
[11] Huang, D., Li, C., Karlas, A., et al. (2025). VibNet: Vibration-boosted needle detection in ultrasound images. *IEEE Transactions on Medical Imaging, 44*(6), 2696–2708.
[12] Asl, M. B., Fofana, I., Meghnefi, F., et al. (2026). Hybrid physics-machine learning diagnostics of transformer winding deformations using FBG sensors. *Electric Power Systems Research, 256*, 112940.
[13] Wang, H., Wang, G., Li, G., et al. (2016). Deep belief network based deterministic and probabilistic wind speed forecasting approach. *Applied Energy, 182*(8), 80–93.
[14] Leuw, B., Badcock, R. A., Chambers, E. V. W., et al. (2026). Progress toward a 10-kA superconducting power supply for levitated dipole reactors. *IEEE Transactions on Applied Superconductivity, 36*(5), 5001006.
[15] Huang, S. R., & Chen, S. Y. (2025). Detection of winding deformations in power transformers from inrush current characteristics using the Chen-Lee chaotic system and Gramian Angular Summation Field. *Chaos, 35*(7), 073104.
[16] Zhao, Z., Tang, C., Chen, Y., et al. (2021). Interpretation of transformer winding deformation fault by the spectral clustering of FRA signature. *International Journal of Electrical Power & Energy Systems, 130*, 106933.
[17] Wang, Y., Zhou, G., Zeng, C., et al. (2021). Research on on-line detection method of transformer winding deformation based on VFTO. *Sensors, 21*(21), 7386.
[18] Li, S., Zhao, D., Wang, X., et al. (2019). Identification of transformer winding deformation fault type based on signal distance and SVM. *IEEE*, 2021–2026.
[19] Wang, M., Yu, Z., & Li, G. (2024). Analytical modeling of short-circuit impedance of square foil winding phase-shifting transformer based on planar energy density equivalence method. *IEEE Transactions on Applied Superconductivity, 34*(8), 5500604.
[20] Shin, S., Lee, H., Song, C., et al. (2025). Evaluation of the applicability of frequency response analysis to rotating electric machines. *IEEE*, 368-374.
[21] Aljohani, O., & Abu-Siada, A. (2016). Application of digital image processing to detect short-circuit turns in power transformers using frequency response analysis. *IEEE Transactions on Industrial Informatics, 12*(6), 2062-2073.
[22] Xu, D. K., & Li, Y. M. (2001). Application research on on-line monitoring of deformation of windings of power transformer. *High Voltage Engineering, 27*(4), 21-22.
[23] Deng, X. L., Xiong, X. F., Gao, L., et al. (2014). Method of on-line monitoring of transformer winding deformation based on parameter identification. *Proceedings of the CSEE, 34*(28), 4950-4958.
[24] Zhang, C. (2007). Test method and its application of transformer winding deformation. *Transformer, 44*(2), 35-37.
[25] Li, C. X., Zhu, T. Y., Yao, C. G., Xia, Q., Mi, Y., & Zhao, Z. Y. (2018). Online diagnosis method for transformer winding deformation based on characteristic of figure constructed by voltage and current. *High Voltage Engineering, 44*(11), 3532–3539.
[26] Liu, M. N., Peng, F. D., Ke, C. J., & Meng, Y. Y. (2012). Diagnosis analysis on transformer winding deformation failure. *Guangdong Electric Power, 25*(11), 108–111.
[27] Zhao, Z. Y., Yao, C. G., Li, C. X., Long, Y., Chen, X. H., & Liao, R. J. (2016). Method for obtaining the impulse frequency response curves of power transformer winding deformation based on short time Fourier transform. *High Voltage Engineering, 42*(1), 241–247.
[28] Nirgude, P. M., Ashokraju, D., et al. (2008). Application of numerical evaluation techniques for interpreting frequency response measurements in power transformers. *IET Science Measurement & Technology, 2*(5), 275–285.
[29] Liu, J. N., Zhao, Z. Y., et al. (2019). Classifying transformer winding deformation fault types and degrees using FRA based on support vector machine. *IEEE Access, 7*, 112494–112504.
[30] Abu-Siada, A., & Islam, S. (2012). A novel online technique to detect power transformer winding faults. *IEEE Transactions on Power Delivery, 27*(2), 849–857.
[31] Li, Y. (2024). Online detection of transformer winding deformation based on DeltaP·U2 improved lissajous plot. *2024 International Conference on Electrical Technology and Automation Engineering, Journal of Physics: Conference Series, 2803*(1), Article 012039 (5 pp.).
[32] Li, Y. N., Yu, H., Peng, W. B., Qian, G. C., Zhu, X. Y., Wang, K., & Peng, B. (2016). A detection method for transformer winding deformations based on the Lissajous graphical characteristics of voltage and current. *Yunnan Electric Power, 44*(3), 25–29.

DOI: 10.54254/2755-2721/2026.35766

[33] Baklanov, D. V., Litvinov, I. I., & Kuparev, M. A. (2018). Power transformer adaptive differential cutoff. *International Journal of Power and Energy Systems, 38*(1), 8–12.
[34] Islam, S. M., & Ledwich, G. (1996). Locating transformer faults through sensitivity analysis of high frequency modeling using transfer function approach. In *Proceedings of the Conference Record of the IEEE International Symposium on Electrical Insulation* (Vol. 1, pp. 38–41).
[35] Minhas, M. S. A., Reynders, J. P., & De Klerk, P. J. (1999). Failures in power system transformers and appropriate monitoring techniques. In *Proceedings of the 11th International Symposium on High Voltage Engineering* (Vol. 1, pp. 94–97).
[36] Reykherdt, A. A., & Davydov, V. (2011). Case studies of factors influencing frequency response analysis measurements and power transformer diagnostics. *IEEE Electrical Insulation Magazine, 27*(1), 22–30.
[37] Firoozi, H., Kharezi, M., Rahimpour, H., & Shams, M. (2011). Transformer fault diagnosis using frequency response analysis—Practical studies. In *Proceedings of the Power and Energy Engineering Conference Asia-Pacific*, 1–4.
[38] Chen, J., Zhaung, Y., Chen, R., et al. (2025). Degree and classification of winding deformation faults based on least-squares fitting of Lissajous trajectory coefficient recognition. In *Proceedings of the International Conference on Information Control, Electrical Engineering and Rail Transit (ICEERT 2023), Lecture Notes in Electrical Engineering (Vol. 1223)*. Springer.